J. exp. Biol. ***180***, 55-73 (1993)
Printed in Great Britain © The Company of Biologists Limited 1993

ANATOMICAL AND PHYSIOLOGICAL IDENTIFICATION OF INHIBITORS OF THE MOTOR GIANT AND SEGMENTAL GIANT NEURONES IN THE CRAYFISH

K. FRASER and W. J. HEITLER

The Gatty Marine Laboratory, School of Biological and Medical Sciences, University of St Andrews, Fife, KY16 8LB, Scotland

Accepted 30 March 1993

Summary

We anatomically and physiologically identify four interneurones which inhibit the motor giant neurone (MoG) and an interneurone which inhibits both the MoG and the segmental giant (SG) neurone of crayfish. We term these the MoG-I1, -I2, -I3, -I4 and MoG/SG-I neurones. MoG-I1 is almost always very strongly dye-coupled to its bilateral homologue. It is one of the interneurones mediating recurrent feedforward inhibition from the giant fibres (GFs) to the MoG. The GFs activate MoG-I1 by a disynaptic path through the SGs (GF → SG → MoG-I1), which is entirely mediated by rectifying electrical synapses. The multisynaptic path (i.e. GF → SG → MoG-I1 → MoG), in which the first two synapses are electrical, ensures reliable and constant short-latency inhibition of the MoGs following their monosynaptic electrical activation by the GFs (GF → MoG). The remaining MoG-Is receive input from the GFs and other sources through unidentified polysynaptic pathways.

Each interneurone inhibits the MoG and/or SG through depolarising IPSPs, which can be as large as 25mV in amplitude. These IPSPs can effectively block transmission from the GFs to the MoG. The unique morphology of the MoG allows the inhibitory connections from the MoG-Is to be visualised at the light microscope level following staining with Lucifer Yellow. The MoG-Is project a high-density cobweb-like network of fine synaptic branches over the surface of the MoG, which spread from the region of the electrical input from the GFs within the connectives, across the expanded integrating region of the MoG, and onto its axon in the proximal region of the third root. The extensiveness of this anatomical connection correlates well with the high effectiveness of the inhibition mediated by some of the MoG-Is.

Introduction

The neuronal circuitry driving the escape tail-flip of Crustacea has been extensively studied at the level of single identified neurones, and it is one of the best understood ‘simple systems’ in the animal kingdom (see, for example, Wine and Krasne, 1982; Wine, 1984). The central feature of the circuit is the two pairs of giant fibre (GF) command neurones, the lateral giant (LG) and medial giant (MG). A spike in the former initiates a

Key words: crayfish, *Pacifastacus leniusculus*, motor giant neurone, segmental giant neurone, tail-flip, escape response, giant fibres, command neurones, electrical synapse, depolarising IPSP, inhibition.

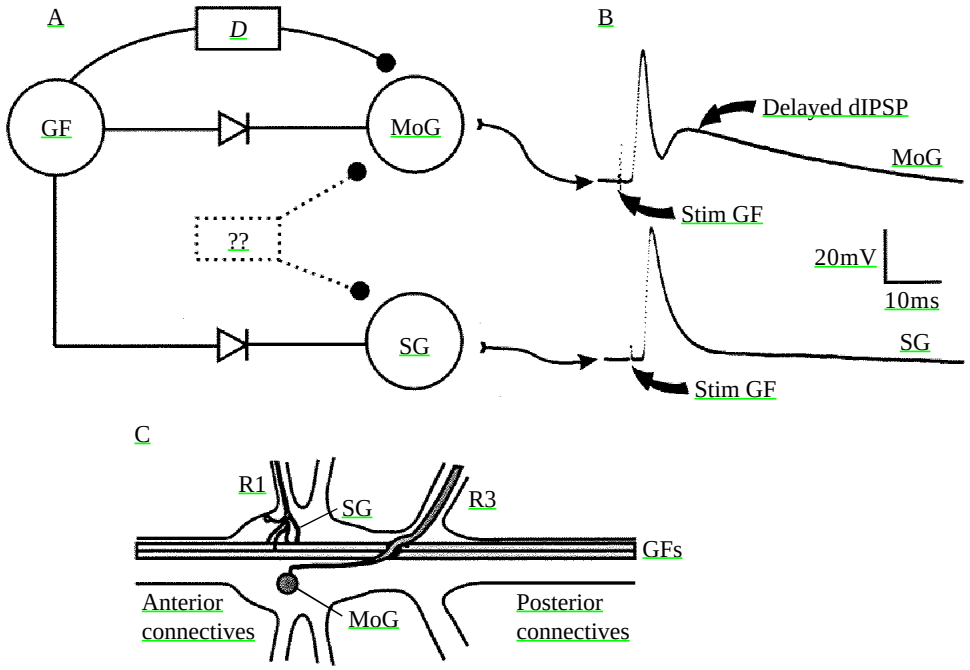

Fig. 1. Summary diagram of previously established circuit. (A) A giant fibre (GF) excites the motor giant neurone (MoG) and the segmental giant neurone (SG) *via* rectifying electrical synapses. The MoG receives delayed recurrent inhibition (*D*) from the GFs, and both the MoG and the SG receive inhibitory input from unidentified sources not directly related to the GF. (B) Examples of MoG and SG response to GF stimulation (Stim). (C) Approximate anatomical relationship between the GFs, MoG and SG within an abdominal ganglion. R1, first root; R3, third root.

tail flexion causing an upward and forward movement of the whole animal, while a spike in the latter initiates a tail flexion causing a backwardly directed movement of the animal.

In the abdomen, the GFs make major output to only two classes of neurone, the motor giant (MoG; Furshpan and Potter, 1959*a*) and segmental giant (SG; Kramer *et al.* 1981). In each case, the output is through rectifying electrical synapses. The MoG is a large abdominal flexor motor neurone, which provides the most important path for flexor motor activity. The SG acts as an interneurone transmitting excitation to the non-giant fast flexor (FF) motor neurones (Roberts *et al.* 1982). The SG is unusual in that, although it has an axon within the first root (R1), this axon is blind-ending and has no output (Heitler and Darrig, 1986).

The only known excitatory input to the MoG and SG in pre-terminal ganglia is from the GFs, but both the MoG and the SG neurones receive considerable inhibitory input. This inhibition exclusively takes the form of depolarising inhibitory postsynaptic potentials (dIPSPs; e.g. Furshpan and Potter, 1959*b*). One frequent source of inhibitory input is feedforward delayed inhibition from the GFs to the MoG (Wine, 1977). The function of this appears to be to prevent multiple spiking of the MoG in response to GF activation. Other inhibitory input is unrelated to GF activity (Fig. 1).

The only MoG inhibitor (MoG-I) that has been fully identified is a local interneurone in the terminal ganglion (G6), which inhibits the MoG in that ganglion (Kirk *et al.* 1986). This inhibitor, called the 'C' neurone because of its shape, is tightly dye-coupled to its contralateral homologue. It receives input from the SG in G6 and also from the corollary discharge interneurones I2 and I3, which originate in G2 and G3 respectively. In pre-terminal ganglia there are thought to be several MoG-I neurones, including some through-conducting interneurones, but they have not been anatomically identified (Wine, 1977). One source of the delayed inhibition of the MoG following a GF spike has been suggested to be the FF motor neurones (Wine, 1977), which are supposed to make central excitatory output to MoG-Is. The evidence for this is that extracellular stimulation of the third root (R3), which contains the axons of the FFs but no sensory neurones, can elicit dIPSPs in the MoG.

In this paper we describe the anatomy and physiology of several MoG-Is, including the pre-terminal homologues of the 'C' neurone, which have been physiologically and anatomically identified by microelectrode recording and staining. We show that one of the paths of MoG inhibition is indeed through the SG, emphasising the role of the latter as a 'driver' interneurone. We further show that there are interneurones that make inhibitory output to both the MoG and SG, and that it is unlikely that the path of excitation of the MoG-Is includes the FF motor neurones.

Materials and methods

Experiments were performed on the central nervous system of the crayfish *Pacifastacus leniusculus* (Dana). Animals were obtained from Riversdale Farm (Stour Provost, Near Gillingham, Dorset, UK). The nerve cord was dissected as follows. An animal was anaesthetised by cooling on ice for 20min, and then decapitated. The legs and chelae were severed at the autotomy plane. The dorsal carapace and viscera were removed, and the nerve cord was dissected from the animal. The last two thoracic ganglia and the entire abdominal chain of ganglia were removed. The nervous tissue was then pinned dorsal surface upwards on a Sylgard platform and submerged in Van Harreveld's crayfish saline.

Bipolar hook electrodes were used to record extracellularly and to stimulate the connectives. Pin electrodes were used to record extracellularly and to stimulate the roots, with a paired indifferent electrode for each pin placed adjacent to it in the preparation bath. Intracellular recordings were made with glass microelectrodes (resistance 15–40 MΩ) filled either with 5% Lucifer Yellow dissolved in 1mol l^{-1} lithium chloride or with 2mol l^{-1} potassium acetate. Penetrations were all made from the dorsal aspect of the ganglion in the axonal or neuropile processes. The ganglionic sheath was removed prior to penetration.

Neurones were injected with Lucifer Yellow using 0.5s negative current pulses of 10–20nA delivered at 1Hz for up to 1h. Preparations were fixed in 5% formaldehyde, dehydrated in alcohol, cleared in methyl salicylate and visualized with a standard epifluorescent microscope.

Results

We have anatomically and physiologically identified four classes of interneurones which inhibit the MoG specifically and one class which inhibits both the MoG and the SG.

Anatomy

MoG-I1: a preterminal homologue of 'C'

We have identified a putative homologue of the G6 'C' neurone (Kirk *et al.* 1986) in G2 (6 preparations) and G3 (14 preparations). We have not examined other pre-terminal abdominal ganglia. Because the name 'interneurone C' has been coined previously for an ascending sensory integrating interneurone of quite different function (Zucker *et al.* 1971), we term the neurone described below MoG-I1.

The anatomy of MoG-I1 is highly distinctive. When a neurone which was suspected to be MoG-I1 was injected with Lucifer Yellow, almost invariably two left–right homologous neurones were revealed (Figs 2, 3). These were so tightly dye-coupled that it was usually impossible to determine visually which neurone had actually been injected (although this could sometimes be determined by electrode position). This is the most complete dye-coupling that we have ever encountered in our studies on crayfish. In only one preparation out of more than 20 in which physiologically identified MoG-I1s have been encountered and stained has a neurone been found with an anatomy suggesting that it was a unilateral MoG-I1.

Each MoG-I1 has a cell body located ventrally just lateral to the midline. A neurite arises from the cell body, ascending towards the dorsal surface and moving slightly anteriorly, and then curves around to the contralateral side of the ganglion. Very extensive dendritic arborizations ramify within the central region of the ganglion, with one major branch extending anteriorly, while another extends posteriorly, giving the pair of coupled neurones an overall H shape. This shape is apparent in photographs taken in the plane of focus of the major dendritic branches (Fig. 2), but is less clear in *camera lucida* drawings, which superimpose all dendrites in the vertical axis (Fig. 3). The posterior branch gives rise to an axon that leaves the ganglion in the lateral margin of the posterior connective.

MoG-I2, -I3 and -I4

MoG-I2 (Fig. 4A) has a cell body located ventrally, just lateral to the midline, in approximately the anterior–posterior middle of the ganglion. A dorsal neurite ascends slightly anteriorly from the cell body and crosses the midline, where dendritic arborizations ramify within the central region of the ganglion, being restricted largely to the side contralateral to the cell body. Two axons arise from this dendritic region, one leaving the ganglion anteriorly, the other posteriorly, each in the approximate middle of the connective. MoG-I2 has been identified in G2 (two preparations) and G3 (four preparations).

Fig. 2. Lucifer Yellow stain of MoG-I1 in G3. Although a single neurone was injected with dye, both bilateral homologues have been stained. The focus is ventral, and the cell bodies are visible, although out of focus. Anterior is at the top. Scale bar, 300 μm.

MoG-I3 (Fig. 4B) has a ventral cell body located halfway between the midline and the lateral margin, towards the anterior end of the ganglion. A neurite ascends posteriorly and gives rise to a thick integrating region, which spans the midline aligned horizontally across the ganglion. An axon arises on the side ipsilateral to the cell body and leaves the ganglion posteriorly. MoG-I3 has been identified in two preparations (G3). In a third preparation (G3), a pair of bilaterally symmetrical homologous neurones was stained, the individual members of which had a structure and physiology similar to MoG-I3. Either this was another neurone entirely or MoG-I3 is sometimes dye-coupled to its contralateral homologue.

MoG-I4 (Fig. 4C) has a ventral cell body in approximately the middle of the hemiganglion. A dorsal neurite gives rise to dendritic branching, which is largely ipsilateral to the cell body but contains some contralateral elements. Two axons arise from these contralateral dendrites, one anterior and one posterior. MoG-I4 has been encountered in three preparation (G3).

Summary of anatomical distinctions

MoG-I1 is easily and unambiguously identified because of its bilateral dye-coupling. Furthermore, it has totally different physiological characteristics from the other MoG-Is (see below). MoG-I2 has an anatomy somewhat similar to MoG-I4, since both have ascending and descending axons with cell bodies contralateral to the axons, but the two neurone types can be distinguished because the dendritic arborization of MoG-I2 is mainly ipsilateral to its axons and rather sparse, while the dendritic arborization of MoG-I4 is more extensive, and is largely contralateral to its axons. MoG-I3 has only a descending axon, and its cell body is ipsilatateral.

Anatomical connections to the MoG

Each MoG-I has a posteriorly directed axon which passes at least to the next posterior ganglion, but we do not know its final termination point. As the axon passes the base of R3, fine branches extend from it and ramify across the surface of the ipsilateral MoG and, in most preparations, also across the surface of the contralateral MoG (Figs 3, 4). The exact morphology of these branches is highly variable, even within a particular class of MoG-I. In some preparations, branches also arise from the axon or dendritic branches at the posterior edge of the ganglion and propagate to the MoG quite separately from the main axon. Sometimes, fine branches arising at the base of R3 may course back into the ganglion and ramify within the ganglionic neuropile. We have not detected any consistent pattern to these detailed branch structures.

The MoG-I branches form a cobweb-like network across the MoG, with expanded bleb-like structures, which are presumably the actual sites of synaptic contact with the

Fig. 5. Enlarged view of the posterior axon of MoG-I2 and the integrating region of the MoG at the base of R3 (see also Fig. 4A). Note the fine branches of MoG-I2 (open arrow) which ramify over the surface of the MoG (filled arrow). The finger-like projections from the MoG, which are the sites of the electrical synaptic input from a GF, are clearly visible (curved arrow). Anterior is at the top. Scale bar, 50 μm.

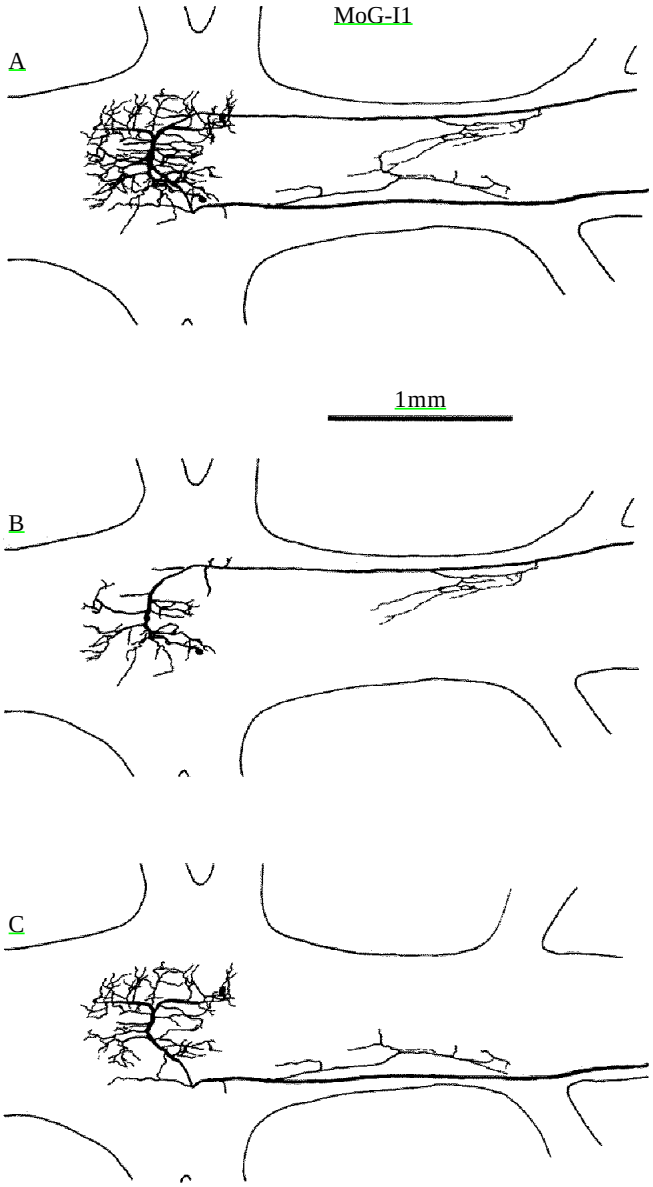

Fig. 3. *Camera lucida* tracing of a Lucifer Yellow stain of MoG-I1. Anterior is to the left. (A) The complete preparation as seen through the microscope, showing the dye-coupled bilateral pair of MoG-I1s. (B,C) The bilateral MoG-I1s are drawn separately, to show the anatomy of the individual neurones. The separation was achieved by following branches from a point unambiguously identified as belonging to one of the two neurones, but since there was no difference in the intensity of staining between the two neurones (see Fig.2), it is possible that some of the finest branches have been assigned to the wrong neurone. It was extremely rare to observe a unilateral MoG-I1 without dye-coupling to its contralateral homologue.

MoG (Fig. 5). These appear to be more or less uniformly distributed across the surface of the MoG, from the finger-like dendritic projections of the MoG, which form the electrical contact with the GFs, out into R3 and the axon proper of the MoG. In one preparation, approximately 120 blebs were counted on a small (0.1mm by 0.23 mm) area of the surface of the MoG. Since the MoG usually has a rather flattened surface after fixation, this suggests a (very approximate) synaptic density of 5000contactsmm^{-2}.

Physiology

MoG-I1

Input to MoG-I1. Extracellular stimulation of a GF in the connectives produces a large (35–50mV), rapidly rising potential in the MoG-I1, which characteristically has one or more 'blips' on the falling phase (Fig. 6A). The response is the same whether the lateral giant or the medial giant is stimulated, and so no distinction is made between these two classes of GF in this report. The GF stimulus also induces spikes in the ipsilateral and contralateral SGs. The SGs can be activated individually by antidromic stimulation of their axons in the first roots (R1) and, when either the left or the right SG is stimulated, MoG-I1 receives rapidly rising depolarising potentials, about 15–25mV in amplitude (Fig. 6B,C). When both SGs are simultaneously antidromically stimulated, the resulting potential in the MoG-I1 is similar in size to that resulting from GF stimulation (not shown). The connection between the SGs and MoG-I1 is *via* rectifying electrical synapses. Depolarising current injected into the SG spreads to MoG-I1 preferentially compared with hyperpolarizing current (Fig. 6D), while hyperpolarizing current injected into the MoG-I1 spreads preferentially to the SG compared with depolarizing current (Fig. 6E).

We attempted to determine whether there was any direct input from a GF to MoG-I1 by removing the intervening SGs through photoinactivation (see Fraser and Heitler, 1991). This confirmed the connection between the SGs and MoG-I1, since during photoinactivation the SG spike underwent massive broadening, leading to a great increase in the input to MoG-I1 (Fig. 7A,B). We were unable to kill the SGs completely (i.e. to abolish their membrane potential) in these experiments because dye-coupling to MoG-I1 invariably developed during the course of the experiment, leading to the start of inactivation of the latter. Nonetheless, we were able to photoinactivate both the SGs to the point where they failed to spike, without noticeably inactivating MoG-I1. When this was done, there still remained a significant input to MoG-I1 in response to GF activation (Fig. 7C). This strongly suggests that there is another input path to MoG-I1 besides that from the homoganglionic SGs. The latency of this input closely matches that of the discontinuity on the falling phase of the MoG-I1 spike in the intact preparation and is probably too long to be a direct monosynaptic input from the GF. In the MoG-I1 of G3, an EPSP was elicited by stimulating the ipsilateral R1 of G2. By analogy with the 'C' neurone of G6, this EPSP might have originated from the corollary discharge interneurone I2 (which would have been activated by the antidromic stimulation of the axon of the SG in G2), and thus the 'blip' on the MoG-I1 spike, and the residual input

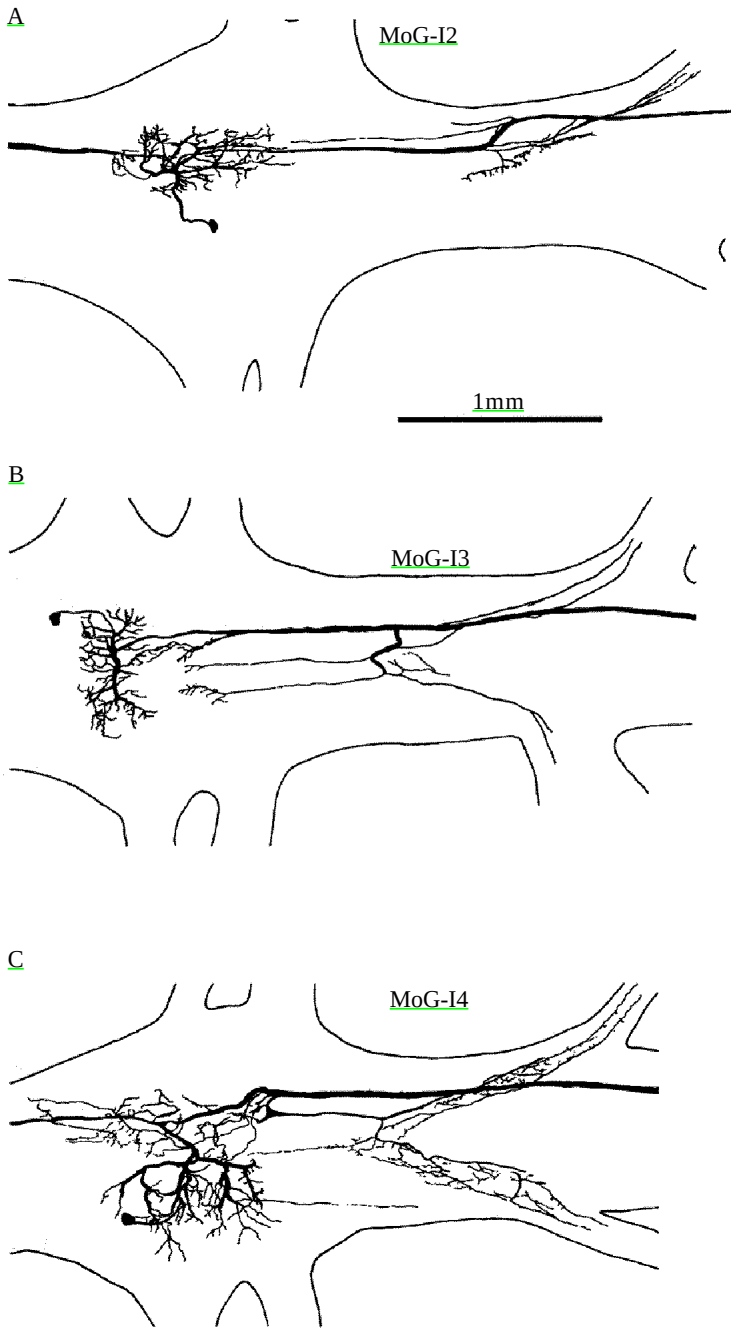

Fig. 4. *Camera lucida* tracings of Lucifer Yellow stains of (A) MoG-I2, (B) MoG-I3 and (C) MoG-I4. For each MoG-I, the anterior ganglionic morphology is shown on the left, while the posterior morphology, at the base of R3, is shown on the right.

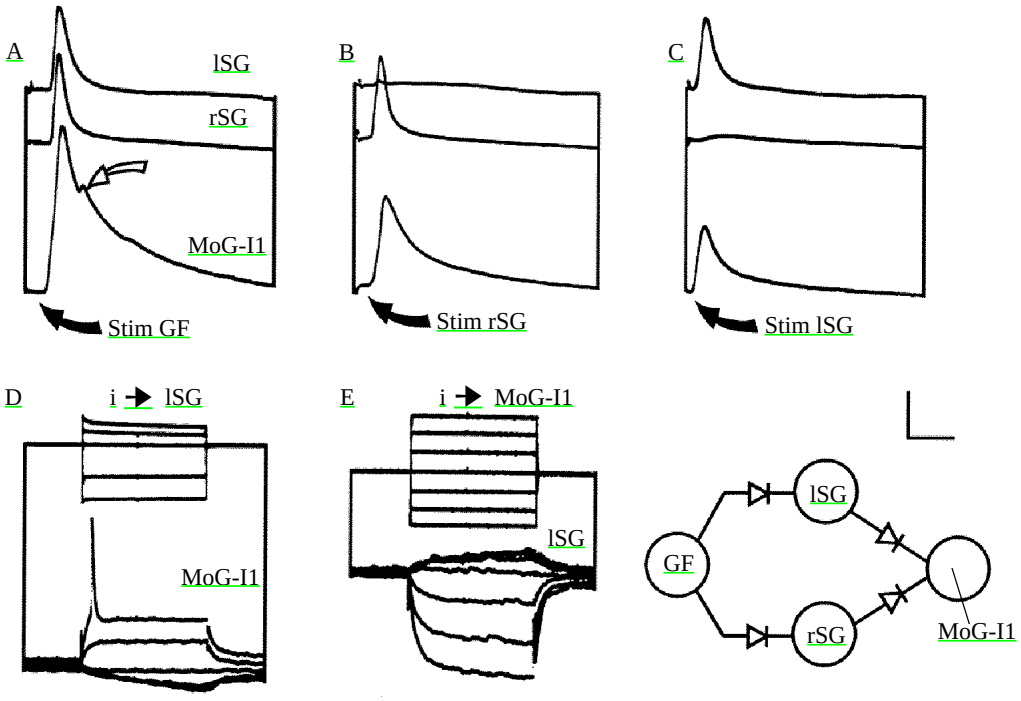

Fig. 6. Input to the MoG-I1 from the GFs is through rectifying electrical synapses *via* the SGs. A–C are from one preparation, D and E are from another, both in G3. (A) Extracellular stimulation (filled arrow) of a GF in the anterior connectives elicits a spike in the lSG (top trace), rSG (second trace) and MoG-I1 (bottom trace). There is a consistent 'blip' on the falling phase of the MoG-I1 spike (open arrow). (B) Extracellular stimulation of the rSG axon in rR1 elicits an antidromic spike in the rSG and a large depolarising potential in the MoG-I1. (C) Extracellular stimulation of the lSG axon in lR1 elicits an antidromic spike in the lSG and a large depolarising potential in the MoG-I1. (D) Depolarising current (top trace monitor) injected (i) into the lSG spreads to the MoG-I1 (bottom trace) preferentially compared with hyperpolarising current. (E) Hyperpolarising current injected into the MoG-I1 spreads preferentially to the lSG compared with depolarising current. Scale bar, vertical SG (A–C) 20mV, (E) 5mV; MoG-I1 (A–C) 10mV, (D) 5mV; current (D) 100nA, (E) 50nA; horizontal (A–C) 5ms, (D,E) 50ms. In this and subsequent diagrams the inset summarises the neuronal circuit. l, left; r, right.

after SG inactivation, could be input from I2. However, we have not confirmed this directly.

MoG-I1 induces dIPSPs in the MoG. MoG-I1 can be induced to spike by injecting it with depolarizing current. Simultaneous recordings from the ipsilateral MoG reveal depolarising synaptic potentials phase-locked to the MoG-I1 spikes (Fig. 8A). Similar phase-locked potentials can also be recorded in the contralateral MoG (Fig. 8B), but we do not know whether this is because each MoG-I1 makes output to both MoGs, or whether the output is strictly ipsilateral, but strong electrical coupling between the bilateral MoG-I1s (as suggested by the dye-coupling) phase-locks their spikes. A spike in the MoG-I1 of G2 has not been observed to produce synaptic potentials in the MoG of G3

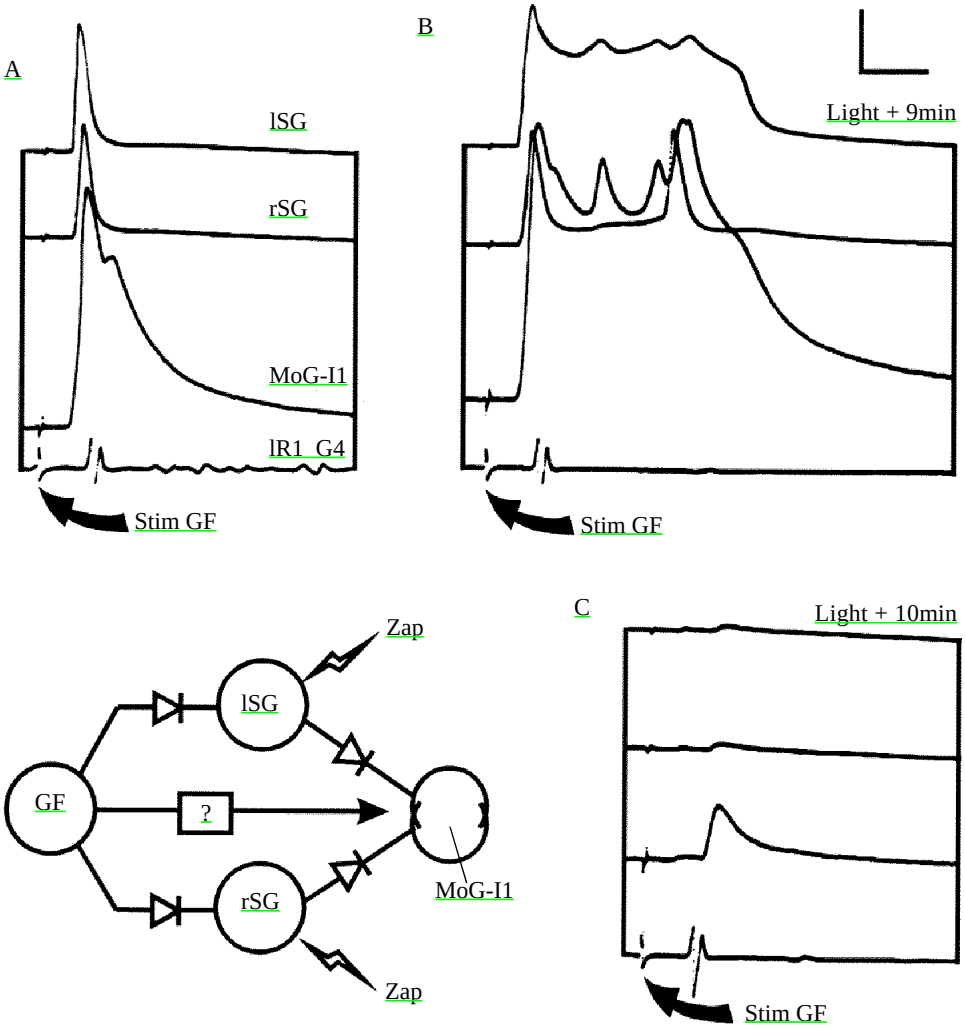

Fig. 7. Photoinactivation of the SGs in G3 reveals a residual input to the MoG-I1 in G3 resulting from GF stimulation. (A) Extracellular stimulation (filled arrow) of a GF in the anterior connective elicits spikes in the lSG (top trace), rSG (second trace) and MoG-I1 (third trace). The spike of lSG in G4 is recorded extracellularly in the lR1 of G4 (bottom trace). Both SGs have been stained with Lucifer Yellow. Note the 'blip' on the falling phase of the MoG-I1 spike (open arrow). (B) The preparation has been exposed to deep blue light (Zap) for 9min. Both SGs have started to photoinactivate, leading to a very broad spike with multiple peaks in each neurone. This, in turn, leads to a very broad spike with multiple peaks in MoG-I1. (C) After 10min of exposure to deep blue light, both SGs have ceased to spike. MoG-I1 no longer spikes in response to GF stimulation, but there is still a substantial EPSP whose latency matches the 'blip' on the spike prior to SG photoinactivation. The SG spike in G4 is unaffected. Scale bar, SG 50mV, MoG-I1 10mV; horizontal 5ms.

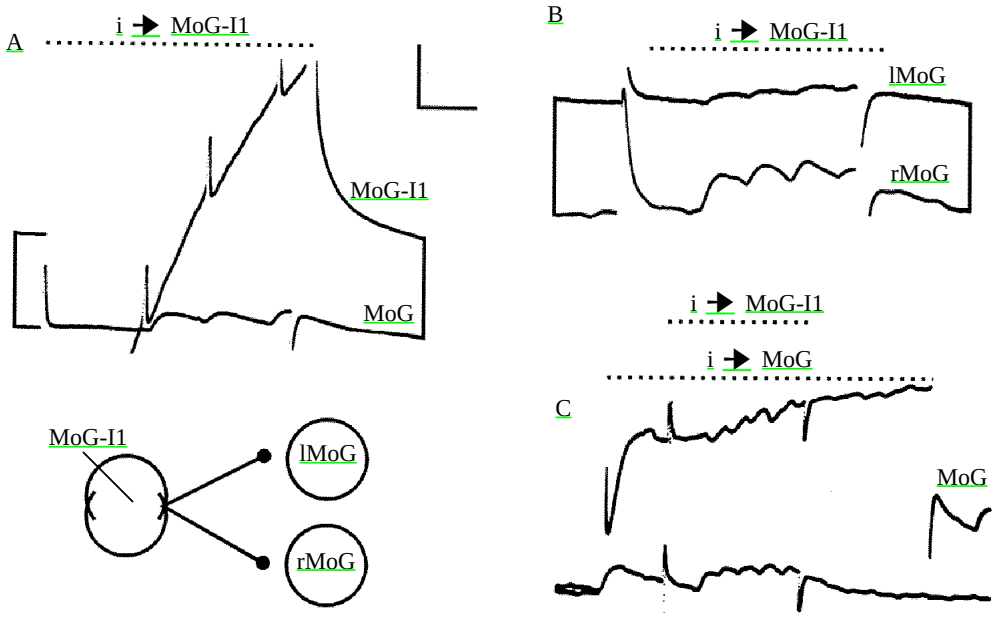

Fig. 8. The MoG-I1 mediates depolarising IPSPs onto the MoG. (A) Depolarising current (dotted line) injected (i) into the MoG-I1 elicits spikes in MoG-I1 (top trace, bridge balance changing during current injection) and phase-locked depolarising potentials in the ipsilateral homoganglionic MoG (bottom trace). (B) Depolarising current injected into the MoG-I1 (not shown) elicits synchronous potentials in the contralateral (top trace) and ipsilateral (bottom trace) homoganglionic MoG. (C) Two sweeps superimposed. In the first sweep, a short pulse of depolarising current (short dotted line) is injected into the MoG-I1 and elicits depolarising potentials in the MoG. In the second sweep the same current is injected into MoG-I1, but it is bracketed by a longer pulse of depolarising current (long dotted line) injected into the MoG. The depolarising potentials are reversed. Scale bar, vertical (A,C) 10mV (B) 5mV; horizontal (A,B) 10ms, (C) 20ms.

(despite the posteriorly directed axon of MoG-I1), although this has only been tested in two preparations. The depolarizing potentials induced in the MoG by MoG-I1 can be inverted by injecting depolarizing current into the MoG through a second microelectrode, showing that they are dIPSPs rather than EPSPs (Fig. 8C).

In a normal preparation, the dIPSPs produced by MoG-I1 are rather small compared with some dIPSPs produced by other MoG-Is (see below). We have never observed the dIPSPs induced in MoG by depolarizing current injected into MoG- I1 to be powerful enough to prevent the MoG from spiking in response to GF activation (e.g. Fig. 9A). However, during the process of photoinactivation, MoG-I1 undergoes massive spike broadening and increases its output considerably (Fraser and Heitler, 1991). Under these circumstances, the dIPSPs summated into a depolarized plateau that almost totally abolished any coincident MoG spikes (Fig. 9B).

MoG-I2–MoG-I4

The physiological characteristics of MoG-I2, -I3 and -I4 are very similar. The data

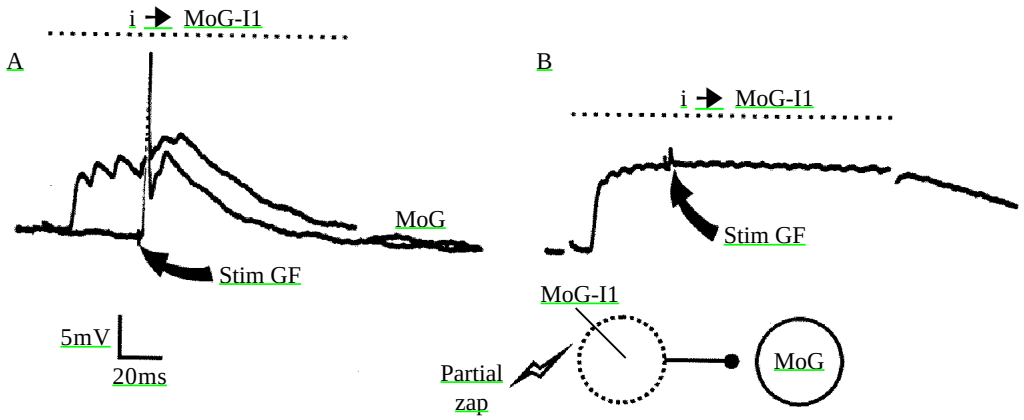

Fig. 9. The dIPSPs mediated by MoG-I1 can inhibit GF–MoG transmission when MoG-I1 spiking is enhanced by partial photoinactivation. (A) Two sweeps are superimposed in a normal preparation. In the first sweep, a GF is activated by extracellular stimulation (curved arrow) of the anterior connective. It elicits a spike followed by a dIPSP in the MoG. In the second sweep, a similar GF activation is bracketed by a pulse of depolarising current (dashed line) injected (i) into the MoG-I1 (not shown). This elicits dIPSPs in the MoG, but does not abolish the MoG spike resulting from GF activation. (B) MoG-I1 has been partially photoinactivated by injecting it with Lucifer Yellow and exposing it to deep blue light (Zap). It now produces a very broad spike with multiple peaks when injected with positive current (not shown, but see Fig. 6B). The dIPSPs in the MoG are massively enhanced and now prevent the MoG spiking in response to GF activation by extracellular stimulation of the connectives.

presented (Fig. 10) are specifically for MoG-I2 but, unless stated to the contrary, apply equally to MoG-I3 and MoG-I4. In each case, spikes can be initiated in the MoG-I by injecting depolarising current and they cause large, sometimes very large (up to 25mV), dIPSPs in the MoG (Fig. 10A). The dIPSPs follow the spikes 1:1, with a fixed latency of approximately 2ms from the peak of the ganglionic spike in the MoG-I to the start of the dIPSP in the MoG at the base of R3 (Fig. 10B). Sometimes, small depolarising potentials can be detected in the LG synchronously with the spikes in MoG-I and the dIPSPs in the MoG (Fig. 10A). These may indicate direct inhibitory input to the LG from MoG-I, since the LG–MoG electrical synapse is strongly rectifying, and it is unlikely that depolarising potentials could spread antidromically back across the synapse. However, the functional significance of this has not been established. When MoG-I2, -I3 or -I4 is induced to spike, small extracellular potentials can usually be recorded in R3 synchronously with the start of the large dIPSPs in the MoG (Fig. 10B). These small extracellular potentials probably originate from spikes in the fine branches of the MoG-Is which propagate into R3 on the surface of the MoG.

The ability of the dIPSPs induced by each of MoG-I2, -I3 and -I4 to inhibit GF–MoG transmission was tested by bracketing extracellular stimulation of the GFs with intracellular stimulation of the MoG-I. The GF stimulation alone induced a spike in the MoG recorded intracellularly, and extracellularly in R3 (Fig. 10C). When the GF stimulation was coincident with dIPSPs caused by the MoG-I, the MoG spike potential

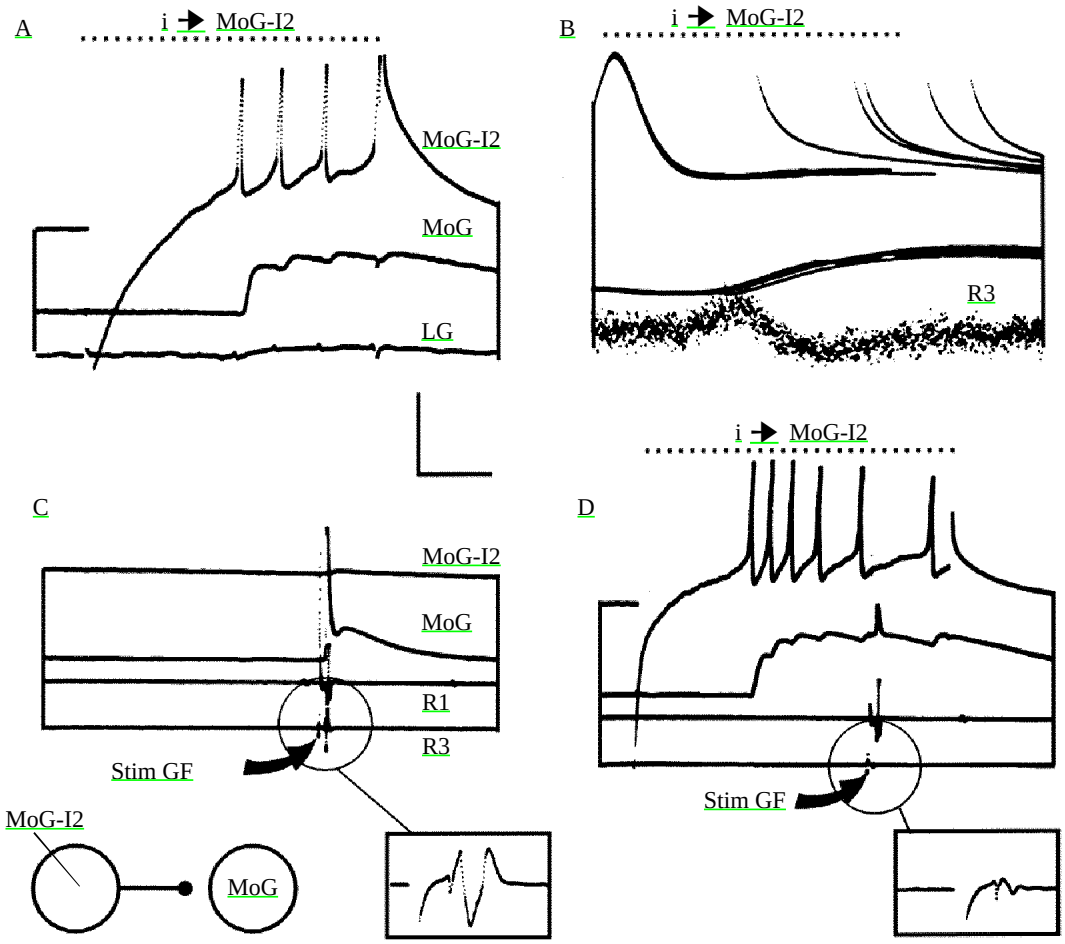

Fig. 10. MoG-I2 initiates large depolarising potentials in the MoG, which can abolish GF–MoG transmission. (A) Depolarising current (dotted line) injected into MoG-I2 (top trace) initiates spikes, and also initiates large depolarising potentials in the MoG (second trace). Small depolarising potentials are also initiated in the ipsilateral LG (bottom trace). (B) Five sweeps superimposed, in which brief depolarising current pulses initiate spikes in the MoG-I2 (top trace) which are used to trigger the oscilloscope. (The falling phase of the membrane potential at the end of the current pulse is visible in several sweeps, following the spike.) Fixed-latency depolarising potentials occur in the MoG (second trace), and a small fixed-latency spike is recorded extracellularly in R3 (bottom trace). This probably originates from fine branches of MoG-I2, which extend over the surface of the MoG into R3. (C) Extracellular stimulation (curved arrow) of a GF in the anterior connectives induces a spike in the MoG (second trace), which is recorded extracellularly in R3 (bottom trace, shown in the inset on an expanded time scale). An SG spike is recorded extracellularly in R1 (third trace). A small depolarising potential is recorded in the MoG-I2 (top trace). (D) As C, except that the GF stimulation is bracketed by depolarising current (dotted line) injected (i) into the MoG-I2. This induces spikes in the MoG-I2 and dIPSPs in the MoG. The GF stimulation no longer initiates a spike in the MoG, and the extracellular MoG spike in R3 disappears (see inset). Note that the extracellular spike of the SG in R1 is unaffected. Scale bar, vertical 20mV; horizontal (A) 10ms, (B) 1ms, (C,D main frame) 20ms, (C,D inset) 2ms.

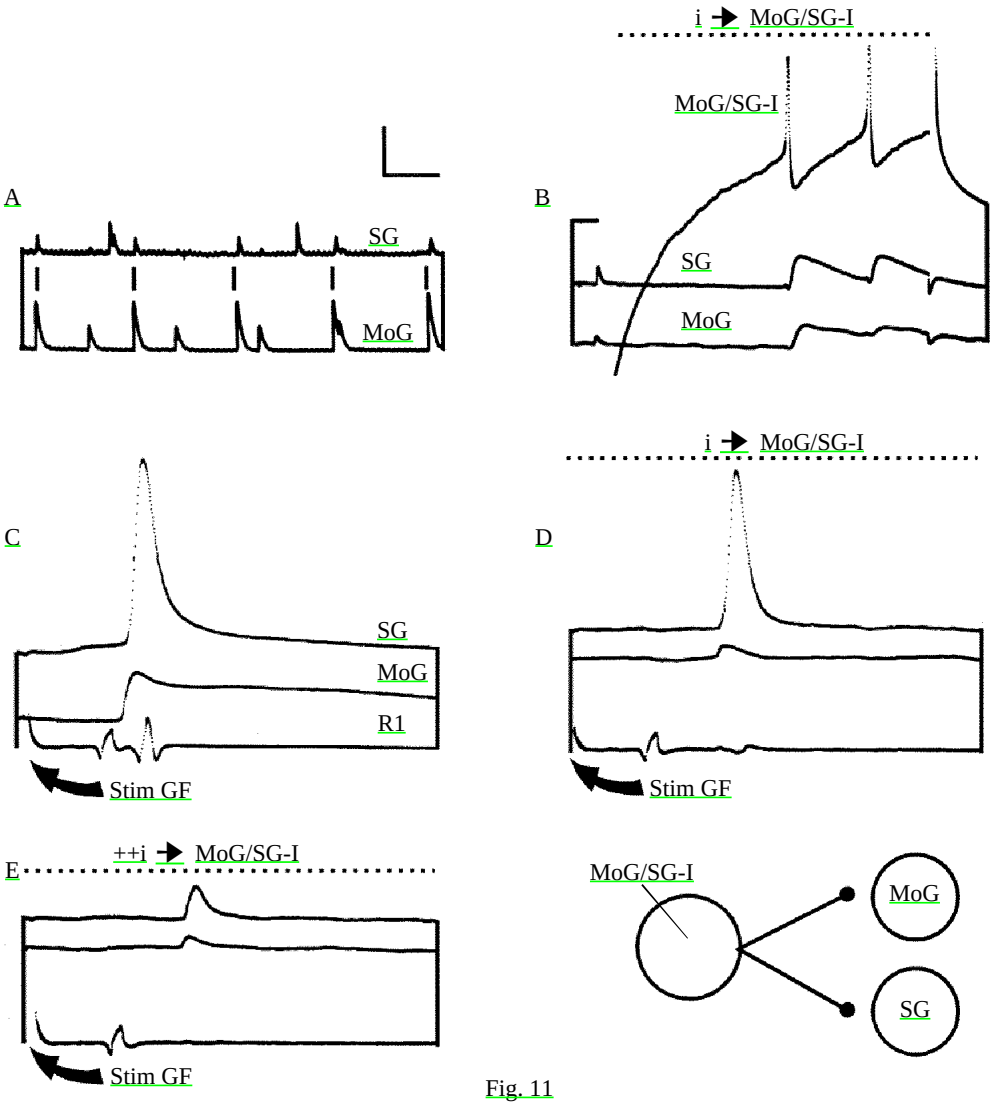

Fig. 11

recorded intracellularly was massively attenuated, and no MoG spike was recorded in R3 (Fig. 10D). In contrast, extracellular recordings from R1 show that the SG axon spike is maintained under conditions where the MoG axon spike is abolished, suggesting that MoG-Is do not make effective inhibitory input to the SG (Fig. 10D).

We have not identified specific paths activating any of MoG-I2, -I3 or -I4. Extracellular stimulation of either the anterior connective between the thorax and G1, or the posterior connective between G5 and G6, initiates EPSPs on each MoG-I, and these can cause spikes, but the spikes do not appear to be antidromic. Extracellular stimulation of R1 initiates smaller EPSPs. Extracellular stimulation of homoganglionic R3 usually initiates a large unitary depolarising potential in each of MoG-I2, -I3 and -I4, with the same stimulus activation threshold as a dIPSP in the MoG. This may indicate that the MoG-Is

Fig. 11. Dual inhibition of the MoG and SG. A is from one preparation, B–E are from another. (A) Simultaneous recordings from the SG (upper trace) and MoG (lower trace) reveal a continuous barrage of depolarising potentials in both neurones. Some potentials are common to the two neurones (vertical lines). (B) A MoG/SG inhibitor (MoG/SG-I; top trace) is injected (i) with depolarising current (dotted lines). Synchronous dIPSPs are recorded in the SG (second trace) and MoG (bottom trace). (C) Extracellular stimulation (curved arrow) of a GF in the anterior connectives induces a spike in the SG (top trace), which is recorded extracellularly in R1 (bottom trace), and an EPSP in the MoG (second trace). There is no response in the MoG/SG inhibitor (not shown). (D) As C, except that the GF stimulation is bracketed by depolarising current (dotted line) injected into the MoG/SG inhibitor (not shown). This induces spikes in the inhibitor and dIPSPs in the MoG and SG. The dIPSPs have summated to a depolarised plateau, and so are not apparent individually. The EPSP in the MoG is strongly attenuated, but the spike in the SG is still present. However, the extracellular SG spike recorded in R1 has disappeared, indicating that the central and peripheral spikes are not absolutely coupled in this neurone. (E) As D, but with more current injected (++i) into the MoG/SG inhibitor. Both the SG spike and the EPSP in the MoG are now inhibited. Scale bar, vertical MoG, SG (B) 10mV, SG (A) 5mV, (B) 10mV, (C–E) 20mV, MoG/SG inhibitor 20mV; horizontal (A) 200ms, (B) 10ms, (C–E) 2ms.

receive input from fast flexor motor neurones activated antidromically (Wine, 1977), but direct activation of individual FF motor neurones by injecting depolarising current (not shown) has never been seen to elicit EPSPs in any MoG-I. In our opinion, the depolarising potentials observed in the MoG-Is resulting from extracellular stimulation of R3 are more likely to result from direct stimulation of the terminals of the MoG-Is in R3 as they spread across the MoG surface. A spike in these terminals could propagate back to the ganglion as an EPSP-like depolarization, due to spike failure at the large discontinuity in diameter where the fine branches join the main axon at the base of R3.

Dual inhibitors of the MoG and SG

Simultaneous intracellular recordings from the SG and MoG show that both neurones frequently receive a barrage of depolarising potentials, and that some are common to the two neurones (Fig. 11A). In seven preparations (five G2, two G3) we have encountered interneurones that activated phase-locked depolarizing synaptic potentials on both the homoganglionic MoG and SG when induced to spike by injecting depolarizing current (e.g. Fig. 11B). In three of these (G2), the interneurone was stained and revealed a through-conducting axon with restricted dendritic arborizations within the ganglion in the region of the SG and at the base of R3. The cell body was not located in the stained ganglion, and hence its position was not determined.

An important question is whether the depolarizing potentials are dIPSPs or EPSPs. In two preparations we were able to show that, by injecting sufficient depolarizing current into the interneurone to induce multiple spiking, the depolarizing synaptic potentials in the MoG could inhibit transmission at the GF–MoG synapse, indicating that they are indeed functional dIPSPs. In these preparations, transmission at the GF–SG synapse was not functionally inhibited at this dIPSP frequency, suggesting that the GF–SG electrical connection is more resistant to modulation than the GF–MoG connection. In a further two preparations, we were unable to demonstrate functional inhibition, but we were able to

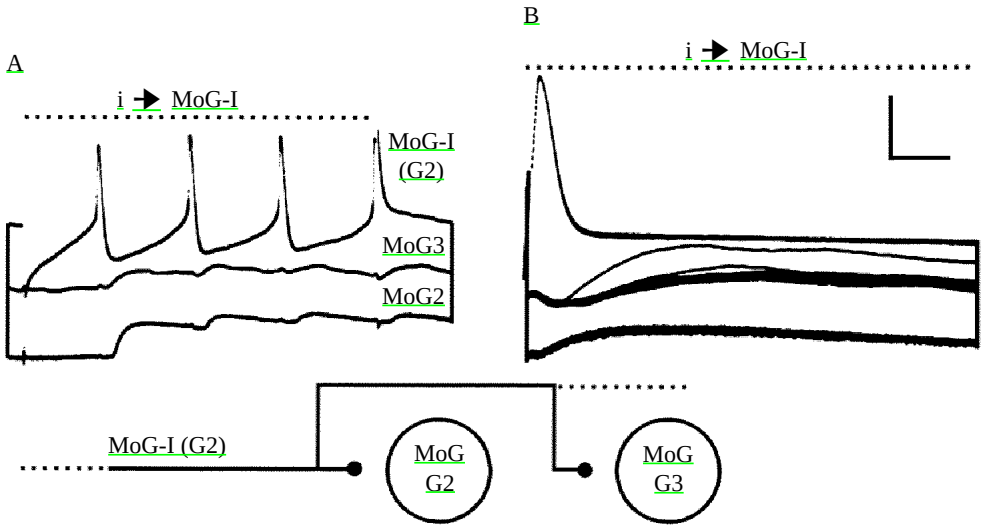

Fig. 12. Multi-segmental inhibitor of the MoG. (A) Depolarising current (dotted line) injected into the inhibitor in G2 (top trace) induces depolarising potentials in the MoG in G2 (bottom trace) and G3 (second trace). (B) As A, but on faster time scale. Multiple sweeps of the oscilloscope are triggered off the spikes in the inhibitor. Scale bar, vertical MoG 5mV, inhibitor 20mV; horizontal (A) 10ms, (B) 2ms.

reverse the polarity of the depolarizing potentials by injecting subthreshold depolarizing current into the MoG, again indicating that the potentials were dIPSPs. In only one preparation were we able to demonstrate functional inhibition of both GF–MoG and GF–SG transmission (Fig. 11C–E). In this preparation, the MoG was not spiking, but its electrical EPSP was massively attenuated by the dIPSPs. The SG spike could also be abolished by superimposing GF stimulation onto dIPSPs induced by depolarising current injected into the MoG/SG-I, but more current had to be injected into the inhibitor to block the SG spike centrally than was required to attenuate the MoG EPSP. Interestingly, the axon spike of the SG recorded extracellularly in R1 was abolished at a *lower* intensity of inhibition than that required to abolish the central SG spike (Fig. 11D,E)

Multi-segmental inhibition of the MoG

There is considerable evidence from earlier work that some through-conducting interneurones mediate multisegmental inhibition onto the MoGs (Wine, 1977). We have not concentrated upon the identification of these interneurones, but have encountered at least one interneurone, which was anatomically similar to one of the MoG–SG inhibitors described above, which induced dIPSPs on both the MoGs of G2 and G3 (Fig. 12).

Discussion

Feedforward inhibition mediated by MoG-I1

In this paper we describe the final links in a complete circuit mediating feedforward

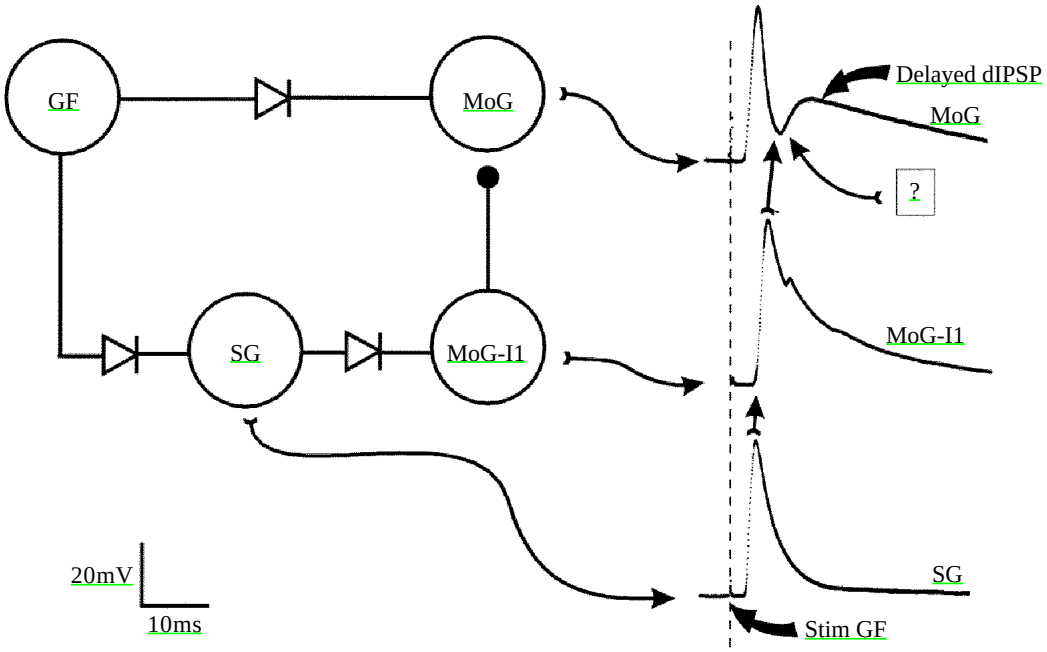

Fig. 13. Summary diagram showing a complete circuit mediating recurrent inhibition from the GFs to the MoG *via* the SGs and MoG-I1. This is the only fully identified circuit, but there are undoubtedly other pathways, as yet unidentified, which mediate recurrent inhibition in parallel to this circuit.

inhibition from the GFs to the MoG (Fig. 13). The GFs have been shown previously to drive the SGs through rectifying electrical synapses (Kramer *et al.* 1981; Roberts *et al.* 1982; Heitler and Darrig, 1986); here we show that the SGs in turn drive the MoG-I1 through rectifying electrical synapses, and that MoG-I1 inhibits the MoG. This is almost certainly not the only pathway which mediates feedforward inhibition (since the dIPSPs that occur on the MoG following GF activation can sometimes be considerably larger than those mediated by MoG-I1), but it is probably one of the most reliable. The GF to SG synapse is extremely stable, and simultaneous spikes in the two bilateral SGs (as would normally occur in response to a GF spike) normally elicit spikes in the MoG-I1. Thus, the activation of the MoG-I1 *via* a disynaptic pathway of powerful electrical synapses ensures that the inhibition of the MoG mediated by the MoG-I1 will reliably arrive at a constant short latency after the GF-activated MoG spike. In our experiments, we found that the dIPSP mediated by MoG-I1 is not strong enough by itself to prevent the MoG from spiking, but the timing of its occurrence, which is tightly controlled by the electrical synapses, ensures that it will augment intrinsic inhibitory cellular events within the MoG (delayed rectification, sodium inactivation, reversed biasing of the rectifying electrical input synapse; Edwards, 1990). It is thus likely to make a significant contribution to the reduced excitability of the MoG following a GF-activated spike.

A major input to MoG-I1 is undoubtedly from the SG neurones. However, non-specific stimulation of the ganglionic roots and connectives shows that there are other unidentified

sources of input. It is thus possible that MoG-I1 may be activated by pathways other than those from the SGs and in circumstances other than GF-mediated escape tail-flips.

We strongly suspect that the MoG-I1 that we describe in this paper is a pre-terminal homologue of the neurone named 'C', which occurs in the terminal abdominal ganglion (Kirk *et al.* 1986). The evidence for this is as follows. (1) The neurones have similar connectivity (input from the SGs, inhibitory output to the MoG). (2) The neurones both occur as a tightly dye-coupled bilateral pair. (3) The cell bodies of the neurones occur in the same relative location. (4) The neurones have dendritic arborizations of broadly similar shape (within the constraints imposed by the terminal location of the C neurone).

Synaptic morphology and inhibitory effectiveness

The dIPSPs mediated by the identified interneurones MoG-I2, -I3 and -I4 can be extremely large (up to 25mV) and are highly effective in preventing GF activation of the MoG. This effectiveness is consistent with the synaptic morphology revealed by staining the MoG-Is. It is extremely unusual to be able to identify sites of synaptic contact at the light microscope level, but the rather simple anatomy of the MoG, which lacks any extensive dendritic arborizations, combined with the location of the MoG-I to MoG synapses at the base of R3, away from the major dendritic neuropile of the ganglion, enables us to visualise the sites of contact in this case (Fig. 5). Dual staining of the MoG-I2 and the MoG shows that the surface of the MoG is covered with a cobweb-like network of synaptic blebs. These extend from the central hemiconnective region, where the GF makes electrical synaptic contact with the MoG, right out along the axon of the MoG into R3. In some cases branches of the inhibitor have been traced as far as the second branch point of R3 as it courses towards the muscle. This extensive area of high-density synaptic contact is the anatomical corollary of the large and effective dIPSPs observed in the MoG in response to activation of the presynaptic inhibitory neurone.

Do the FFs mediate excitation to the MoG-Is?

It has been suggested previously (Wine, 1977) that one pathway mediating feedforward excitation of the MoG-Is from the GFs is *via* the fast flexor (FF) motor neurones. The evidence for this was that stimulating R3, which contains the axons of the FFs, induced dIPSPs in the MoG. Consistent with this, we have found that stimulating R3 extracellularly can induce depolarising potentials in MoG-Is. However, we have never observed dIPSPs arising in the MoG as a result of specific intracellular stimulation of any FF motor neurone, nor have we observed EPSPs in any MoG-I arising from this stimulation (K. Fraser and W. J. Heitler, unpublished data). Furthermore, in this paper we show that small potentials can be recorded extracellularly from R3; these are phase-locked to spikes in the MoG-Is when the latter are induced by intracellular current injection. It is perhaps possible that these might be field potentials arising from the large dIPSPs occurring on the MoG, and propagating by cable conduction some distance along R3, but a more likely explanation is that they are spike potentials arising from branches of the MoG-Is which themselves extend out into R3. The reason we favour this explanation is that Lucifer Yellow stainings of MoG-Is show that such branches do indeed frequently occur. When R3 is stimulated extracellularly with pulses of increasing amplitude, the

initial response in a MoG-I is usually a depolarising potential, which then shows stepped increments in amplitude as the stimulus is increased, eventually giving rise to a spike. We interpret this as being due to progressive recruitment of spikes in the fine branches of the MoG-I, until the summed branch-spike current is sufficient to propagate a spike antidromically past the expansion in axon diameter that occurs at the base of R3.

This work was supported by a grant to W.J.H. from the Science and Engineering Research Council of the UK, and from the Hasselblad Foundation.

References

EDWARDS, D. H. (1990). Mechanisms of depolarizing inhibition at the crayfish giant motor synapse. I. Electrophysiology. *J. Neurophysiol.* **64**, 532–540.

FRASER, K. AND HEITLER, W. J. (1991). Photoinactivation of the crayfish segmental giant neurone reveals a direct giant-fibre to fast-flexor connexion with a chemical component. *J. Neurosci.* **11**, 59–71.

FURSHPAN, E. J. AND POTTER, D. D. (1959*a*). Transmission at the giant motor synapses of the crayfish. *J. Physiol., Lond.* **145**, 289–325.

FURSHPAN, E. J. AND POTTER, D. D. (1959*b*). Slow post-synaptic potentials recorded from the giant motor fibre of the crayfish. *J. Physiol., Lond.* **145**, 326–335.

HEITLER, W. J. AND DARRIG, S. (1986). The segmental giant neurone of the signal crayfish and its interactions with abdominal fast flexor and swimmeret motor neurones. *J. exp. Biol.* **121**, 55–75.

KIRK, M. D., DUMONT, J. P. C. AND WINE, J. J. (1986). Local inhibitor of the crayfish telson-flexor motor giant: anatomy: morphology and physiology. *J. comp. Physiol.* A **158**, 69–79.

KRAMER, A. P., KRASNE, F. B. AND WINE, J. J. (1981). Interneurons between giant axons and motoneurons in crayfish escape circuitry. *J. Neurophysiol.* **45**, 550–573.

ROBERTS, A., KRASNE, F. B., HAGIWARA, G., WINE, J. J. AND KRAMER, A. P. (1982). Segmental giant: evidence for a driver neuron interposed between command and motor neurons in the crayfish escape system. *J. Neurophysiol.* **47**, 761–781.

WINE, J. J. (1977). Neuronal organization of crayfish escape behavior: inhibition of giant motoneuron *via* a disynaptic pathway from other motoneurons. *J. Neurophysiol.* **40**, 1078–1097.

WINE, J. J. (1984). The structural basis of an innate behavioural pattern. *J. exp. Biol.* **112**, 283–319.

WINE, J. J. AND KRASNE, F. B. (1982). The cellular organization of the crayfish escape behaviour. In *Biology of Crustacea*, vol. III, *Neural Integration* (ed. H. Atwood and D. Sandeman), chapter 15. New York: Academic Press.

ZUCKER, R. A., KENNEDY, D. AND SELVERSTON, A. I. (1971). Neuronal circuit mediating escape responses in crayfish. *Science* **173**, 645–650.

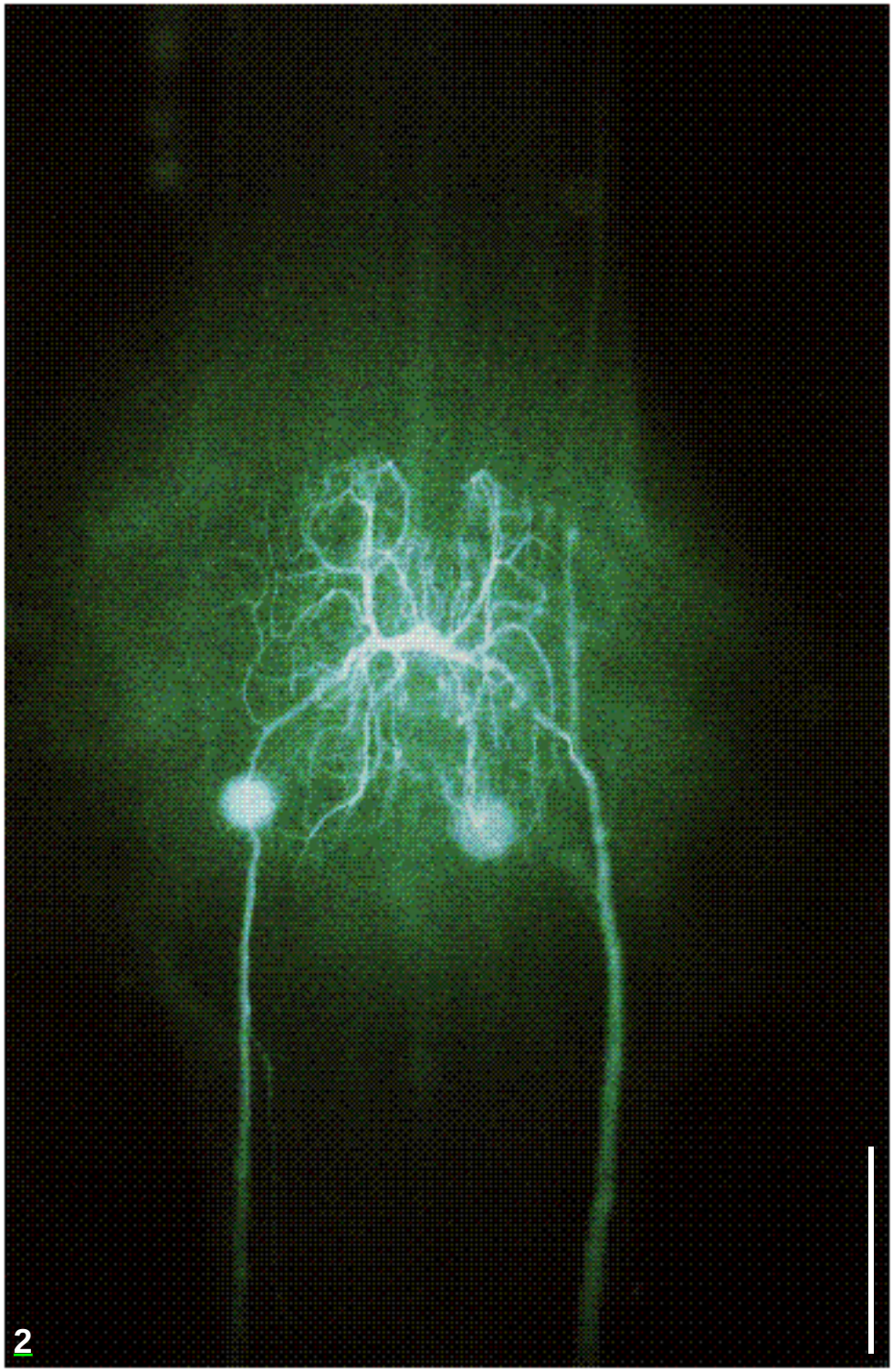
2

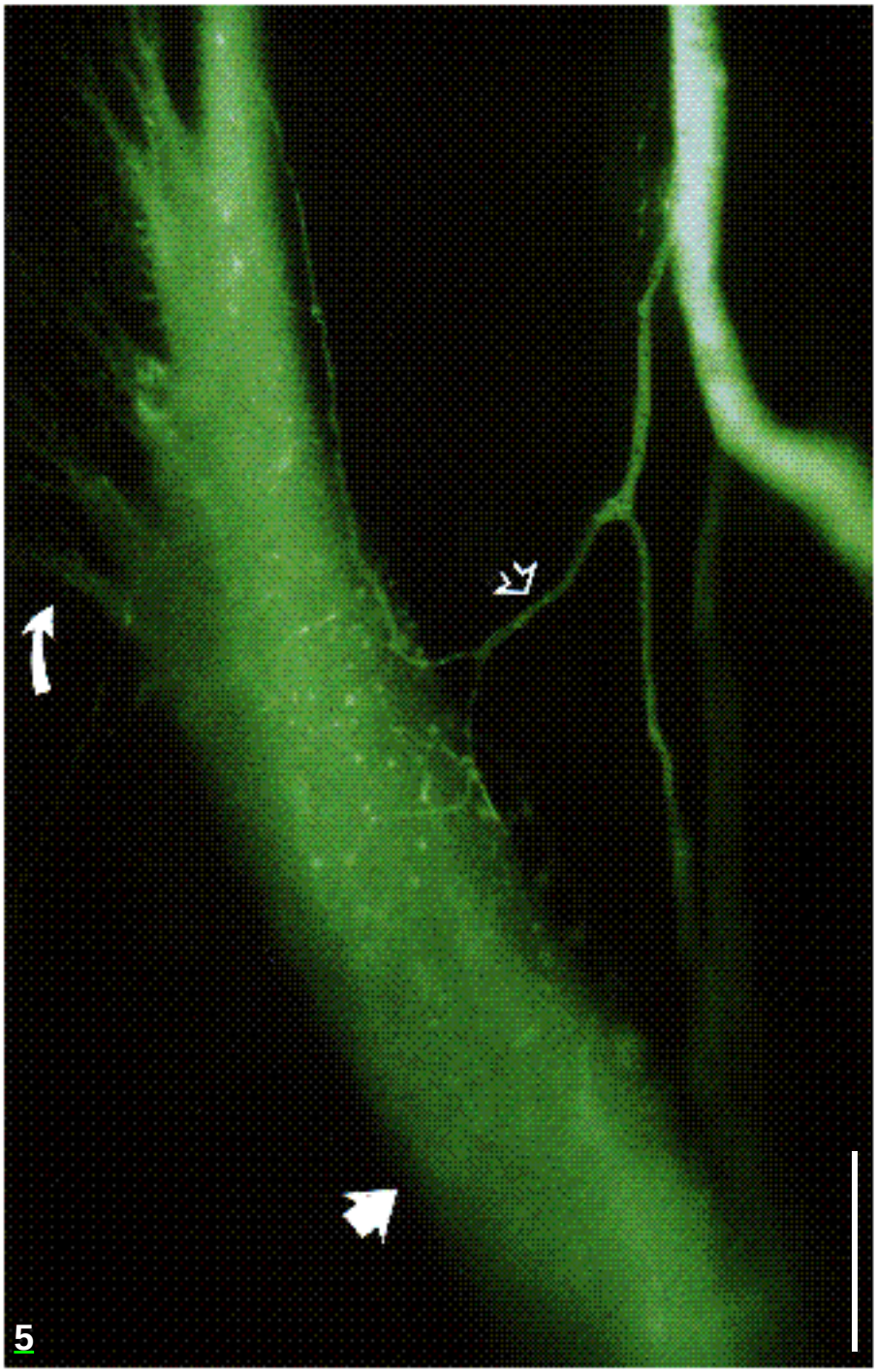
5